RATE-SENSITIVE CONSTITUTIVE AND FAILURE PROPERTIES OF HUMAN COLLATERAL KNEE LIGAMENTS

J. R. Kerrigan, B. J. Ivarsson, D. Bose, N. J. Madeley,
S. A. Millington, K. S. Bhalla, J. R. Crandall
University of Virginia Center for Applied Biomechanics

ABSTRACT
Current finite element models of the human lower extremity lack the accurate constitutive representations of knee ligaments necessary for computational evaluation of pedestrian injury countermeasures. The collateral ligaments have been reported to be the most frequently injured knee ligaments in pedestrians involved in automobile collisions. The purpose of this study is to determine the material and failure properties of human collateral knee ligaments tested in tension to failure at two different rates. Four lateral collateral ligament (LCL) specimens and 4 medial collateral ligament (MCL) specimens are tested to failure in tension at a high rate (1600 mm/s), and 4 LCL and 4 MCL specimens are tested to failure at a low rate (1.6 mm/s). Each specimen consists of a bone-ligament-bone complex and the tensile direction is representative of joint distraction at 0° flexion. 3-dimensional non-contact surface digitization is used to calculate the cross sectional area of each ligament. The Lagrangian strain of the surface of the ligament is calculated by speckle pattern motion recognition. The average LCL ultimate stress and elastic modulus (39.3 MPa and 477.9 MPa, respectively) are more than double the ultimate stress and elastic modulus of the MCL (15.98 and 138.3, respectively). The data show that in both ligament types, the stress at a particular strain in an average high rate test is significantly greater than the stress at the same strain in an average low rate test ($p<0.001$), proving the presence of rate sensitivity over the range of strain-rates examined (1%/s-2400%/s).

Keywords: Knee, Ligaments, MCL, LCL, Constitutive Properties, Pedestrian

PEDESTRIAN-AUTOMOBILE COLLISIONS (PACs) cause as many as 8,000 fatalities and 300,000 injuries to vulnerable road users (VRU) in the European Union each year (Commission of the European Communities-CEC, 2003). In the United States, there were almost 5,000 VRU fatalities and another 78,000 VRUs were injured in PACs in 2001 (NHTSA, 2001). The CEC has published a proposal for a directive that will require new automobiles sold in the European Union to incorporate measures aimed to mitigate injuries to pedestrians involved in PACs (CEC, 2003). The proposal calls for full implementation of acceptance testing for all new vehicles by 2015. One of these acceptance tests assesses the potential for injury to the pedestrian lower limb in the event of impact with the bumper.

In anticipation of the proposed regulations, automobile manufacturers are currently designing and testing front end components in an attempt to bring their platforms within compliance. Since testing on post-mortem human surrogates (PMHS) can be logistically difficult and very costly, some automobile manufacturers prefer computational modeling for evaluation of proposed pedestrian injury countermeasures. As a result, several research groups have developed finite element (FE) models of the human lower extremity for evaluation of potential pedestrian injury countermeasures (Bermond *et al.*, 1993, 1994; Yang *et al.*, 1996; Schuster *et al.*, 2000; Takashashi *et al.*, 2000, 2003; Beillas *et al.*, 2001 and Maeno *et al.*, 2001). Rapid advances in computational modeling have made it possible to incorporate increased complexity in the constitutive representations of soft tissues. Since knee

ligaments play a central role in knee-joint and lower limb kinematics, their constitutive properties are critical in FE analysis.

The structural and material properties of human knee ligaments have been studied for decades, with most work focusing on the cruciate ligaments due to the frequent occurrence of sports injuries involving the cruciates (Trent *et al.* 1976, Kennedy *et al.* 1976, Noyes & Grood 1976, Tremblay *et al.* 1979, Piziali *et al.* 1980, Marinozzi *et al.* 1983, Butler *et al.* 1986, Hollis *et al.* 1988, Rauch *et al.* 1988, Woo *et al.* 1991, Jones *et al.* 1995, and Rowden *et al.* 1997).

However, in PACs accurate representations of the collateral ligaments are most crucial to modeling joint kinematics and predicting injury. Of the 357 PAC cases surveyed by Teresinski and Madro (2001), 165 (46%) of the pedestrians were struck on the lateral (or medial) side. 80% of all of the pedestrians included in the study, and 94% of those sustaining a lateral impact, sustained injuries to the knee ligaments or femoral/tibial epiphyses. Varus-valgus strain has been identified by Teresinski and Madro as the most common mechanism for knee injury in pedestrians hit from the lateral or medial side (Teresinski and Madro, 2001). The collateral ligaments are the most commonly injured ligamentous structures when the knee sustains a varus-valgus strain (Kajzer *et al.*, 1990, 1993, 1997, 1999; Bhalla *et al.* 2003, Kerrigan *et al.* 2003, Teresinski, 2003). Thus the accuracy of the constitutive representations that model the response of the collateral ligaments is crucial for FE-based pedestrian injury countermeasure development and evaluation. These constitutive representations must be derived from results obtained in experimental testing of collateral ligaments.

There are, however, only a few published studies aimed at characterizing the structural or material properties of the human collateral ligaments (Table 1). Three studies report the structural properties of the collateral ligaments (Trent *et al.* 1976, Kennedy *et al.* 1976, Marinozzi *et al.* 1983). Although the failure data from these three studies appear to be in general agreement, direct comparison is difficult due to the difference in ages of the PMHS and applied load rates. There are two studies that report material properties of human collateral knee ligaments (Butler *et al.* 1986, Quapp and Weiss 1998). Butler *et al.* 1986 reports data from tests on bone-ligament-bone specimens of the anterior cruciate ligament (ACL), posterior cruciate ligament (PCL) and the LCL averaged together. Quapp and Weiss (1998) tested dog-bone shaped cut-outs of the MCL by applying a tensile force parallel to the long axis of the individual fibers.

Table 1. Selected data from previous studies on the structural and material properties of human collateral knee ligaments.

		Trent et al. (1976)	Kennedy et al. (1976)	Marinozzi et al. (1983)	Butler et al. (1986)*	Quapp and Weiss (1998)
	PMHS Age	29-55	20-75	55-90	21-30	62 ± 18
	Load Rate	DNR	2 mm/s 8 mm/s	1.7 mm/s	100% strain/s	1% strain/s
MCL	**Ultimate Load (N)**	516 ± 222	468 ± 106 665 ± 236	465 ± 190	-	DNR
MCL	**Stiffness (N/mm)**	71 ± 16	DNR	60 ± 22	-	DNR
MCL	**% Elongation**	DNR	23 ± 8 24 ± 4	13 ± 6 %	-	17 ± 2
MCL	**Ultimate Stress (N/mm^2)**	-	-	-	-	39 ± 5
MCL	**Elastic Modulus (N/mm^2)**	-	-	-	-	332 ± 58
LCL	**Ultimate Load (N)**	377 ± 191	-	425 ± 95	DNR	-
LCL	**Stiffness (N/mm)**	60 ± 42	-	60 ± 22	DNR	-
LCL	**% Elongation**	DNR	-	19 ± 8 %	15 ± 4	-
LCL	**Ultimate Stress (N/mm^2)**	-	-	-	36 ± 12	-
LCL	**Elastic Modulus (N/mm^2)**	-	-	-	345 ± 107	-

* ---Butler et al. reports the results from tests with the LCL, ACL, and PCL together.

\- ---Non applicable (Did not test or measure)

DNR ---Does not report

The ligament properties determined in the studies mentioned above are inadequate for FE simulation of pedestrian impact kinematics due to the low strain-rate as well as the strain and cross sectional area measurement methodologies. Unpublished finite element simulations of lateral impact PACs at 40 km/h predict that collateral ligaments are strained at 3000-5000%/s (Takahashi *et al.* 2002). All of the experimental studies mentioned above report tests conducted at rates at least an order of magnitude less than that. The tests reported by Butler *et al*. (1986) were performed at rates closest to the rates predicted by the unpublished FE study, however Butler *et al.* (1986) used a constant pressure area micrometer to measure the cross sectional area and a vernier caliper to measure the length of each bundle used in strain calculations. Traditional instruments for measuring the dimensions of soft-tissues, such as calipers, introduce error due to tissue deformation (Lee and Woo, 1988) and also require the assumption of a regular cross sectional shape (rectangular, as in Quapp and Weiss, 1998, circular, or ellipsoid as in Haut and Little, 1969). Devices like area micrometers standardize the shape of the cross section and pressure applied, yet underestimate the area due to deformation; a result of the applied pressure (Allard *et al.* 1979). Non contact methods such as laser micrometry (Lee and Woo, 1988, Iconis *et al.* 1987) provide better accuracy but are unable to account for surface concavities.

METHODS

In the current study, 8 MCL and 8 LCL specimens were ramped to failure in the vertical distraction orientation (Figure 1) in displacement control. Four MCL specimens and four LCL specimens were tested at high rate (1600 mm/s) and the rest were tested at low rate (1.6 mm/s). Ligament cross sectional area, determined from an advanced non-contact surface digitization system, was used to convert resultant load to stress. Lagrangian strain of the ligament surface was calculated by tracking surface speckle motion. Ultimate force, Lagrangian strain and stress at the time of the ultimate force, the linearized elastic modulus, the linearized distraction stiffness, the Lagrangian strain-rate and the cross sectional area for 13 of the 16 ligaments are reported in this study.

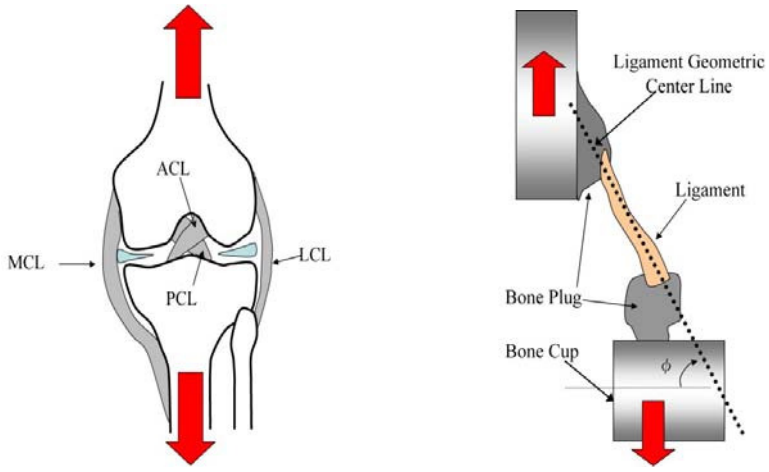

Figure 1. Schematic representations of the vertical distraction orientation in which ligaments in this study were tested. The vertical distraction orientation is defined by applying displacements to the knee joint along the axis of the tibia. Since the ligament long axis is not parallel to this direction, achieving this orientation required transverse displacement of one of the bone plugs. The schematic on the right shows an example of how a potted specimen might look in its testing orientation. The ligament geometric center line is inclined at the elevation angle φ. *The schematic on the right is not meant to actually depict the distraction orientation for either of the collateral knee ligaments*.

SPECIMEN PREPARATION: Six male PMHS were obtained and used in accordance with local and federal laws, as well as with the ethical guidelines and research protocol approved by the Human Usage Review Panel and a University of Virginia institutional review board. Pretest CT scans verified the absence of bone or joint pathology. The PMHS were refrigerated (2° C) within 3-4 days and frozen (<-10° C) within one week postmortem. All limbs were sectioned prior to thawing and defrosted individually in temperature controlled water for 24 hours prior to ligament specimen

preparation (Table 2). Each bone-ligament-bone specimen was extracted and potted by an orthopaedist.

Table 2. Anthropometry for the 8 lower limb specimens tested in this study (L denotes the left limb, R denotes right limb).

Specimen	Age	Height (cm)	Weight (kg)
149L/R	40	170.2	94.8
162L	43	188.0	113.4
161L	61	182.9	65.8
169L	62	170.2	61.2
135R	63	172.7	68.9
159L/R	66	167.6	65.8

Each lower limb specimen was carefully dissected free of all tissue except for the bones and the four major ligaments. At this time, the location and orientation of the distal insertion with respect to its proximal insertion for each collateral ligament was recorded so that the same orientation could be reproduced during potting and subsequent testing.

First the proximal tibiofibular joint was disarticulated and the fibula was cut off 4-6 cm inferior to the ligament insertion. The proximal MCL and LCL bone plugs were obtained by bisecting the medial and lateral femoral condyles, respectively, in the sagittal plane. The tibia was then cut 4-6 cm inferior to the most distal fiber insertion of the MCL and the tibia was then split in a sagittal plane. This allowed for potting without damage to the ligament. Small holes were drilled in the bone plugs and a single screw was inserted through each plug. Both the screw and the holes served to increase the contact area between the bone and the potting material. The specimens were potted in small aluminum cups using R1 Fast Cast No. 891 (Goldenwest Mfg; Inc., Cedar Ridge, CA USA), a fast setting urethane casting resin. Special care was taken to ensure that no resin came in contact with ligamentous tissue and that the bone plugs were cast in the proper anatomical orientation.

All ligament specimens were kept moist during the extraction and subsequent potting using physiological 0.9% saline. After the potting, the specimens were wrapped in saline soaked gauze, individually sealed and "snap" frozen from room temperature to -60 ^{o}C in approximately 60 seconds using liquid CO_2. The specimens remained at room temperature for dissection and preparation for no more than 4 hours.

TEST BATTERY: Twelve to twenty-four hours prior to each test, the test specimen was allowed to thaw at 2 ^{o}C. Before testing, the specimen was removed from the refrigerator and submerged in saline (at room temperature) for a minimum of 15 minutes. The ligament cross section and length measurements were then made using a caliper to provide a rough estimate of ligament size variation. Two length measurements were made (shortest and longest) parallel to the ligament long-axis. The mass of the entire specimen (bone-ligament-bone, potting, and potting cups) was recorded using a digital scale. The specimen was then mounted in a test fixture that was attached to the cross head of the actuator of an Instron 8800 servo hydraulic biaxial test machine (Instron, Canton, MA, USA).

The test fixture (Figure 2) allowed the rotation of the specimen about the axis of displacement. The rotation was necessary to perform the surface digitization. A rotational bearing at the fixture base was connected by shafts to the biaxial actuator (rotation and vertical motion) of the test machine. An x-y table mounted on the rotational bearing permitted displacements of the tibial/fibular bone cup (always mounted on the bottom) in the transverse plane. A 6 axis load cell (R. A. Denton, Rochester Hills, MI, USA) was mounted on top of the x-y table for measuring resultant force through the ligament. The bone cups were clamped in specially designed latching cup mounts, which provided a secure grip on the cup and the block of urethane resin. The top latching cup mount, was mounted below a plate that was guided on the shafts that connected the actuator to the rotational bearing. Low friction bearings attached to the plate permitted easy slippage over the shafts during vertical displacement of the actuator. The vertical displacement of the actuator was measured by both a string potentiometer and the linear-variable-differential-transformer (LVDT) of the test machine. An accelerometer was mounted on the actuator to record its acceleration during the high rate (~1600 mm/s) tests. A three-accelerometer array was mounted on the bottom latching mount cup to record any vibrations of the

load cell and latching mount cup. The acceleration data were used to inertially compensate load signals from the 6-axis load cell. Finally a load cell (Instron Dynacell, Instron, Canton, MA, USA) was mounted between the actuator and the top plate to provide a live readout of the vertical force in the ligament.

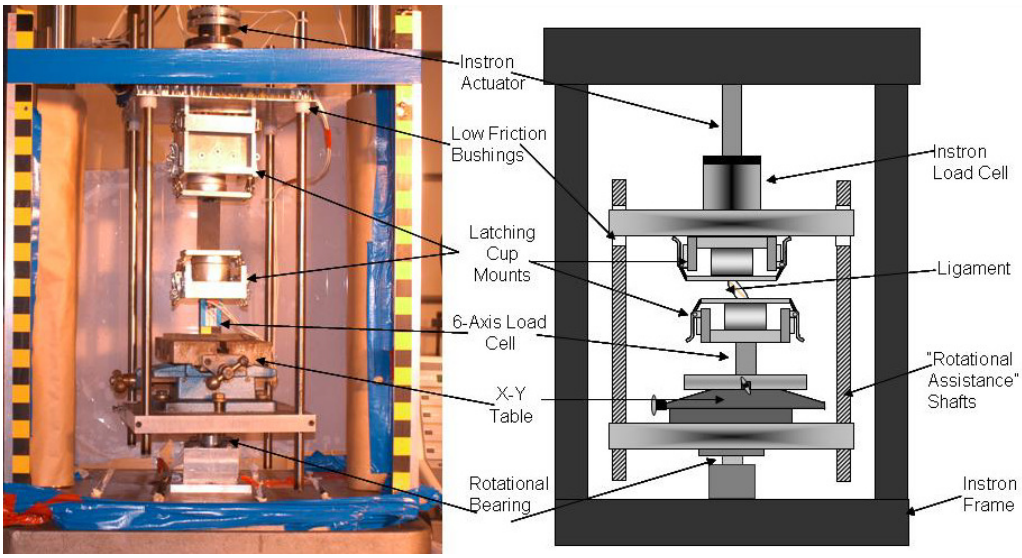

Figure 2. A photograph of the test fixture is shown on the left (a piece of rubber is used to simulate a ligament in this picture). A schematic of the test fixture is shown on the right .

Once the specimen was mounted, the relative transverse displacement (defining the distraction orientation) measured by the orthopaedist surgeon during specimen preparation was applied to the distal bone cup. The ligament was aggressively sprayed with room temperature physiological (0.9%) saline every 5-15 minutes during testing.

The unpreconditioned zero strain position was determined by lowering the actuator until there was no load on the ligament, and then raising the actuator until the vertical tensile load through the ligament measured 2 N (Funk *et al.* 2000). The ligament was then preconditioned by applying 40 cycles of a sinusoidal displacement at 8 Hz. A preliminary (unpublished) experimental study suggests that 40 cycles is the average number of preconditioning cycles necessary to achieve a constant cyclic hysteresis loss in collateral knee ligaments. It was desired to not strain the ligament to a point that may cause any macro or micro-failures of the structure during the preconditioning. Thus the vertical amplitude of the actuator during the preconditioning test was defined as an amplitude that would produce a 10% normal strain (linear displacement ratio) in the ligament (Funk, 2000). The vertical displacement, d, required to produce a normal linear strain, E, in a structure of length, l, leaning at an initial elevation angle, φ^0, can be shown to be

$$d = l\left(-\sin\left(\varphi^0\right)+\sqrt{\sin^2\varphi^0 + E(E+2)}\right) \quad (1)$$

The preconditioning amplitude for each specimen was calculated from the shortest gage length of the ligament (measured with calipers parallel to the long-axis of the ligament) and the initial elevation angle (calculated from the gage length and relative transverse displacements that defined the distraction orientation).

After the preconditioning, the ligament was allowed to relax for a minimum of 20 minutes in a slacked position. Preliminary (unpublished) experimental work performed by our group suggests that 20 minutes is the average amount of time it takes for the force relaxation to decrease below 1%/minute during a step-and-hold test on a collateral ligament. A new zero strain position (preconditioned zero strain) was then determined, as described above. The new zero strain position was necessary since the measured load after at the unpreconditioned level was less than 2 N.

Lagrangian strain in the direction of the ligament long axis (as defined by the line connecting the centers of the insertions) was calculated by tracking the motions of paint speckles on the surface of the ligament during loading. But since these data had to be related to actuator displacement to provide instantaneous strain values, a Lagrangian strain-actuator displacement (LSAD) relationship was

determined through pattern recognition using digital imaging ("strain-pictures"). At this time, five quasi-static steps in displacement were applied to the ligament at 40%, 60%, 70%, 88% and 100% of the actuator amplitude during preconditioning. It is important to note that these displacements are simple percentages of vertical actuator preconditioning amplitude and they, therefore, do not cause normal linear strains in the ligaments of 4%, 6%, 7%, 8.8% and 10%.

Before the displacement steps were applied, a paint speckle pattern was sprayed onto the ligament surface (Figure 3). At the zero strain level and at each of the displacement steps, a high-resolution digital photograph (10-11 pixels per mm) was taken. For the LCL , the photographs were taken from a lateral angle perpendicular to the plane defined by the ligament long axis and the direction of actuator displacement (such that the ligament elevation angle φ—see Figure 1—was at a maximum). Due to the flat-thin structure of the MCL, the photographs were always taken from the medial aspect of the ligament. Each of the strain-pictures were processed to track the displacements of the speckles during the quasi-static displacements of the actuator. The coordinate displacement of the speckle pattern was used to determine the relationship between actuator displacement and Lagrangian strain (LSAD) of the ligament.

Figure 3. The left image is a digital photograph of an MCL specimen at the zero strain position. The image on the right is a photograph of a LCL specimen at the zero strain position.

After the strain-pictures, the ligament was allowed to relax for 20 minutes. A new zero strain position was then determined (as described earlier). A non-contact three dimensional digitizer (ATOS^{TM}: Advanced TOpometric Sensor) was then used to compute the surface geometry of the ligaments. The digitizer uses the principle of structured lighting to obtain explicit information about the ligament surface structure. A series of phase shifted fringe patterns were projected on the ligament and imaged using two CCD (charge coupled device) cameras to yield spatial coordinates of the surface. Many images, each from a different lateral aspect of the ligament, were obtained to generate the 3-dimensional model. Reference markers on the test fixture were used to ensure overlap between successive measurements. The system yielded detailed point cloud data, which were processed to develop a solid model of the ligament. The resolution of point spacing in the digitized model ranges from 0.03 mm to 0.15 mm. (see Bose *et al.* 2002 for a more detailed methodology).

After the surface digitization, a new zero strain position was again determined to prepare for the failure test. While ramping to failure, in the low rate tests (1.6 mm/s), high resolution photographs were taken at a rate of approximately 2 images/s to provide more data points for defining the LSAD relationship. Before the high rate (~1600 mm/s) tests, the actuator was lowered to put slack in the ligament. Since it was desired to have the load applied to the ligament at constant velocity, slacking the ligament as much as possible allowed the actuator to accelerate to constant velocity before any load was applied to the ligament. High-speed video (1000 frames/s) was taken of the specimen during the failure. After the test, the ligament failure mode was documented. Multiple linear regression analyses of the failure data for the LCL and the MCL were performed on the stress-strain curves from the failure tests to determine the significance of rate sensitivity.

DATA PROCESSING: Data from all sensors (all 7 load channels, the string potentiometer, the test machine LVDT, and all 4 accelerometers) were sampled at 1 kHz during preconditioning , at 20 Hz during the strain-pictures, at 10 kHz during the high rate failure tests and at 200 Hz during the low rate failure tests. Preconditioning data were examined to verify that the cyclic hysteresis loss was constant by the 40th cycle and to verify that there were no appreciable failures of the ligament structure during the cyclic loading. Actuator displacement data from the strain-pictures tests were used to verify the actuator position in each of the pictures.

Ligament surface digitization data were used to calculate the unloaded ligament cross-sectional area. The solid model was sliced perpendicular to the long axis of the ligament and the cross sectional area was computed using Green's theorem (Bose *et al.* 2002). Instantaneous stress values were calculated as the ratio of the instantaneous force to the unloaded cross sectional area of the ligament.

From the photographs obtained during the strain-pictures test, the same 4 speckles were identified in each of the 6 pictures. These four speckles defined two vectors, *u* and *v*, and the vectors were never parallel nor perpendicular to each other. For each of the five pairs of images (a pair consisted of the zero strain or first picture and one of the pictures taken after a displacement step was applied), the elements of the deformation gradient *F* were calculated as

$$\begin{bmatrix} u_x^* \\ u_y^* \end{bmatrix} = \begin{bmatrix} F_{xx} & F_{xy} \\ F_{yx} & F_{yy} \end{bmatrix} \begin{bmatrix} u_x \\ u_y \end{bmatrix} \text{ and } \begin{bmatrix} v_x^* \\ v_y^* \end{bmatrix} = \begin{bmatrix} F_{xx} & F_{xy} \\ F_{yx} & F_{yy} \end{bmatrix} \begin{bmatrix} v_x \\ v_y \end{bmatrix} \tag{2a}$$

$$[F] = \begin{bmatrix} F_{xx} \\ F_{xy} \\ F_{yx} \\ F_{yy} \end{bmatrix} = \begin{bmatrix} u_x & u_y & 0 & 0 \\ 0 & 0 & u_x & u_y \\ v_x & v_y & 0 & 0 \\ 0 & 0 & v_x & v_y \end{bmatrix}^{-1} \begin{bmatrix} u_x^* \\ u_y^* \\ v_x^* \\ v_y^* \end{bmatrix} \tag{2b}$$

where u_x, u_y, v_x and v_y denote the components of the vectors *u* and *v* in the 0 strain image (the unstrained vectors), and u_x*, u_y*, v_x* and v_y* denote the components of the vectors *u* and *v* in the other image of the pair (the strained vectors). The five Lagrangian strain tensors, *E**, were then calculated as

$$E_k^* = \frac{1}{2}\left(F_k^T F_k - I\right) \quad k = 1..5 \tag{3}$$

from the deformation gradient *F* calculated for each of the five pairs of images. Then a coordinate system rotation transformation was applied to each tensor to rotate one of the normal Lagrangian strain components such that it was in the same direction as the ligament long axis by

$$\overline{E}_k^* = Q^T E_k^* Q \qquad k = 1..5 \tag{4}$$

where $\bar{E}_k$* is the transformed tensor, *Q* is the transformation (or cosine) tensor, and Q^T denotes the transpose of the transformation tensor.

The strain along the axis of the ligament (the transformed Lagrangian strain tensor) from each image defined one point of the LSAD relationship. Thus each ligament had a minimum of five points to define this relationship (but most of the low rate tests had many more from the photographs taken during the ramp-to-failure test). It can be shown that the Lagrangian strain *E**(*d*) in a straight two-dimensional body, that is initially at an angle φ^0 to the vertical, varies according to the expression

$$E^*(d) = \frac{\sin\varphi^0}{l} d + \frac{1}{2l^2} d^2 \tag{5}$$

where *l* is the original (unloaded) length of the ligament measured along its long axis and *d* is the vertical displacement of the upper end of the body (note: Equation 5 is not the inverse of Equation 1; Equation 5 uses a Lagrangian strain model whereas Equation 1 uses a normal linear strain model). Since it is difficult to accurately measure the original length of the ligament, the data points were fit using a least square algorithm to the function

$$E^*(d) = \alpha d + \beta d^2 \tag{6}$$

where α and β are constants that are determined by the least square algorithm. Equation 6 is the LSAD relationship as it was used to convert all displacement measurements to Lagrangian strain measurements for the ramp-to-failure test.

The three acceleration signals measured on the lower latching mount cup were used to inertially compensate the three force components measured by the 6-axis load cell (see Figure 2) in the high rate ramp-to-failure tests. This was necessary because the acceleration pulse that was imparted to the actuator of the test machine during the high rate tests caused the entire system to vibrate. The inertial compensation mass was estimated to be composed of the lower latching mount, ½ of the load cell mass, and ½ of the mass of the specimen and potting. The inertial mass ranged from 1100 g to 1250 g. Once the inertial compensation of the load signals was performed, no data signals exhibited any cyclic behavior; therefore additional signal filtering was unnecessary (all signals were hardware filtered with a 3300 Hz anti-aliasing filter as they were collected).

RESULTS

The data from three specimens were not included in this study due to failures during the preconditioning and a bone failure within the potting. The 7 remaining LCL specimens failed in the ligamentous tissue just proximal to the fibular insertion (Figure 4). The 6 remaining MCL specimens failed in the mid-substance of the ligamentous tissue in close proximity to the meniscal attachment (Figure 4).

Ligament surface digitization yielded the ability to draw ligament contours in any direction (Figure 5). Cross sectional area differed widely between the specimens for both the MCL and the LCL (Table 3). The average (±S.D.) cross sectional area for the MCL and LCL was 88.8±38.5 mm^2 and 15.3±7.9 mm^2, respectively.

Figure 4. Post failure photographs of an MCL (left) and an LCL (right). All of the MCLs in this study had failures that initiated either just inferior or just superior to the meniscal insertion. All of the LCLs in this study had failures that initiated just superior to the fibular insertion.

Figure 5. Detailed point cloud data from the surface digitization of an MCL (left) and an LCL (right) yield three dimensional contours that can be drawn in any direction. These contours are drawn perpendicular to the long axis of the ligament.

Table 3. Failure data for each test with averages and standard deviations by ligament type and actuator displacement rate.

Test #	Spec. #	Spec Type	Actuator Displacement Rate* (mm/s)	Max Force (N)	Lagrangian Strain @ Max Force	Stress @ Max Force (MPa)	Linearized Elastic Modulus** (MPa)	Linearized Distraction Stiffness*,*** (N/mm)	Lagrangian Strain-rate*** (% / s)	Cross Sectional Area (mm^2)
L1	161L	LCL	1.6	269.3	6.98%	35.72	538.5	34.2	1.35%	7.54
L2	149R	LCL	1.6	359.7	6.48%	15.44	261.7	52.6	1.38%	23.29
L3	162L	LCL	1.6	466.0	8.42%	17.49	230.4	58.5	1.52%	26.64
L4	169L	LCL	1.6	453.4	6.69%	26.01	436.4	66.5	1.40%	17.43
			AVERAGE	**387.1**	**7.14%**	**23.67**	**366.8**	**52.9**	**1.41%**	**18.73**
			S.D.	**91.7**	**0.88%**	**9.25**	**146.0**	**13.7**	**0.07%**	**8.37**
L5	159L	LCL	1600	583.5	5.25%	34.76	742.8	80.7	1029.20%	16.79
L6	149L	LCL	1600	417.7	12.50%	59.59	485.0	49.4	2224.15%	7.01
L7	135R	LCL	1600	712.2	13.72%	86.11	650.3	80.6	2470.68%	8.27
			AVERAGE	**571.1**	**10.49%**	**60.15**	**626.0**	**70.2**	**1908.01%**	**10.69**
			S.D.	**147.6**	**4.58%**	**25.68**	**130.6**	**18.0**	**770.99%**	**5.32**
M1	161L	MCL	1.6	1004.3	20.04%	10.87	71.3	70.2	1.93%	92.40
M2	149R	MCL	1.6	1359.4	24.37%	8.36	40.1	82.3	2.02%	162.57
M3	162L	MCL	1.6	1551.2	16.55%	25.93	170.7	88.3	1.38%	59.82
			AVERAGE	**1305.0**	**20.32%**	**15.05**	**94.0**	**80.3**	**1.78%**	**104.93**
			S.D.	**277.5**	**3.92%**	**9.50**	**68.2**	**9.2**	**0.35%**	**52.51**
M4	159L	MCL	1600	1068.4	8.91%	13.79	174.8	88.4	1033.17%	77.47
M5	169L	MCL	1600	1121.2	7.89%	19.22	264.4	98.1	1022.72%	58.34
M6	135R	MCL	1600	1454.2	17.61%	17.71	108.5	86.1	1558.00%	82.11
			AVERAGE	**1214.6**	**11.47%**	**16.91**	**182.5**	**90.8**	**1204.63%**	**72.64**
			S.D.	**209.2**	**5.34%**	**2.80**	**78.2**	**6.4**	**306.07%**	**12.60**

*--Pertaining to displacements applied to the specimen in the distraction orientation (parallel to the long axis of the tibia).
**--Averaged over the linear part of the loading curve
***--Averaged over the time from the onset of load until the time the peak force was recorded

The least square algorithm used to calculate the LSAD relationship yielded good fits to each data set (Figure 6). The values of the constants α and β for each ligament specimen are not given here because they are specific to the orientation in which the ligament was tested. Normal linearized strain typically overestimated the Lagrangian strain, and sometimes by as much as 7 or 8%. This is why some specimens were able to be preconditioned to 10% linearized strain and still failed below 10% Lagrangian strain.

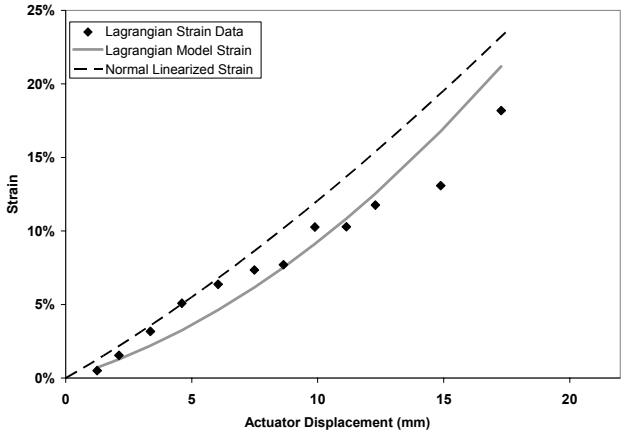

Figure 6. Example of LSAD fit of data points obtained from images taken during the quasi-static displacement steps and during the ramp to failure of one of the MCLs. For comparison, the normal linearized strain, calculated by inverting Equation 1, is plotted (dotted line). This strain was calculated using the shortest length of the ligament (measured by calipers perpendicular to the long axis of the ligament) and the transverse displacement values, measured by the orthopaedist, used to define the distraction orientation. The normal linearized strain consistently overestimates the ligament Lagrangian strain.

Most of the ligament properties vary widely within each of the four test groups (Table 3). Results of the multiple linear regression analysis show a significantly higher mean stress (averaged over the loading curve to failure) for the MCLs tested at the high rate (Figure 7) as compared to the MCLs tested at the low rate (95% confidence interval: 2.93-4.20 MPa, $p<0.001$). The multiple regression analysis performed on the LCL data shows that the mean stress in those specimens tested at high rate (Figure 8) is significantly higher than the mean stress in the those tested at the low rate (95% confidence interval: 15.34-16.70 MPa, $p<0.001$).

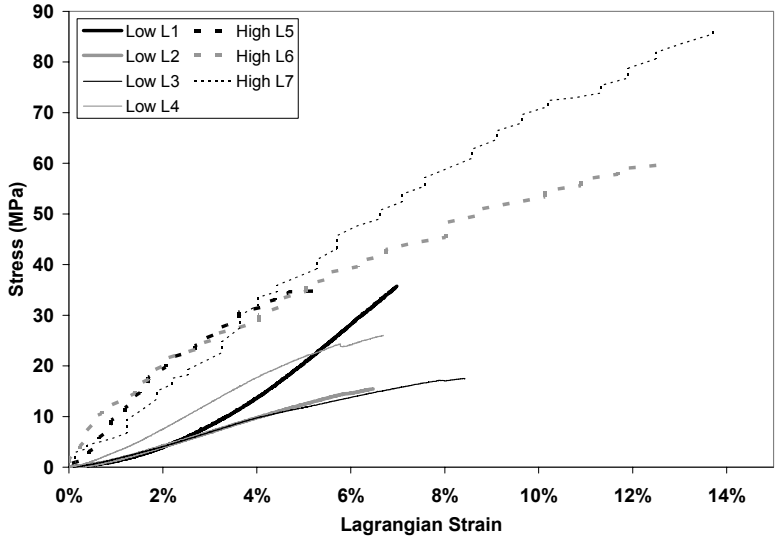

Figure 7. Ligament stress as a function of ligament surface Lagrangian strain for the tested LCLs. The terms "High" and "Low" refer to the rate at which the ligament was ramped-to-failure. The mean stress in the LCLs tested at the high rate is significantly higher than in the LCLs tested at the low rate.

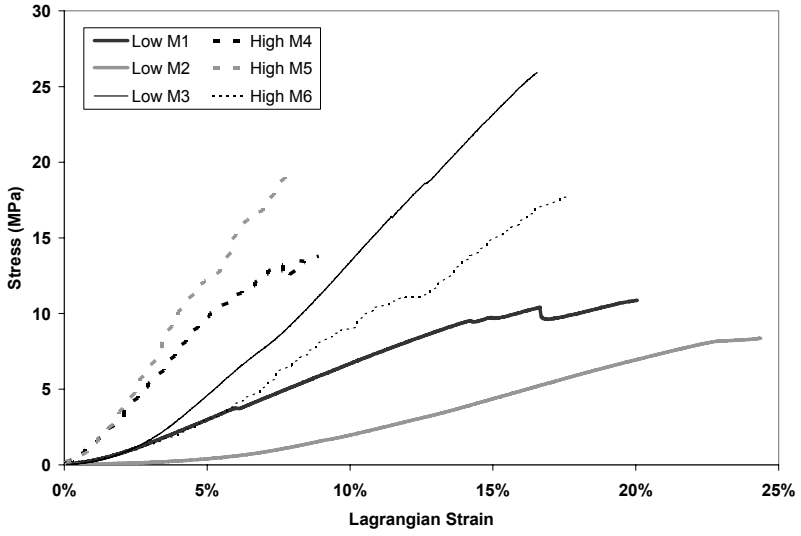

Figure 8. Ligament stress as a function of ligament surface Lagrangian strain for the tested MCLs. The terms "High" and "Low" refer to the rate at which the ligament was ramped-to-failure. The mean stress in the MCLs tested at the high rate is significantly higher than in the MCLs tested at the low rate.

DISCUSSION

There were four criteria imposed for not including a specific specimen's test results in this study. Tests were abandoned:

1) if the failure mechanism was a bone fracture or a failure of the potting to hold the bone end motionless during the test,

2) if the load curve from the preconditioning was not smooth (denoting a premature tissue failure due to the preconditioning amplitude),
3) if the actuator position at the preconditioned zero strain level differed from the actuator position at the unpreconditioned zero strain level by more than 1.5 mm (again denoting a tissue failure as a result of the preconditioning amplitude), or
4) if the actuator position at the zero strain level after the strain pictures or after the surface digitization differed from the actuator position at the preconditioned zero strain level by more than 0.5 mm.

Two specimens (1 MCL and 1 LCL) were discarded due to the third criteria. Both the discarded specimens were from the same limb. These specimens were the only two that had been refrigerated for longer than 24 hours prior to testing, which may have lead to degeneration of the specimens. No specimens were discarded as a result of the second criteria (Figure 9). Therefore, the preconditioning amplitude used in this study is not so high as to cause failures in collateral knee ligaments tested in distraction at 0° flexion. Additionally, one specimen was rejected on the basis of the first criteria and none were rejected on the basis of the fourth criteria. During the test of the specimen abandoned for the first criteria, the tibial bone piece (the specimen was an MCL) made a cracking sound during the preconditioning, and during the failure test the bone fractured below the potting level.

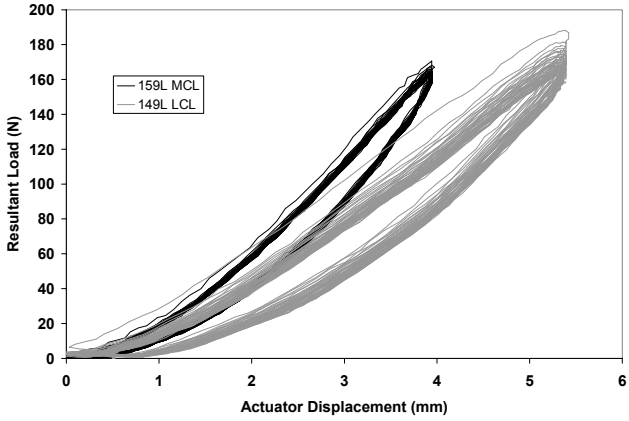

Figure 9. Hysteresis plots from an example MCL and an example LCL. A sharp drop in the load, usually during the first preconditioning cycle, typically indicates a failure of the tissue caused by preconditioning to too high an amplitude. None such failures were observed in any of the tests presented in this study.

Interestingly, all of the other MCL specimens and all of the other LCL specimens failed at the same place in the ligament (MCL specimens failed very close to the meniscal insertion and all of the LCL specimens failed very close to the fibular insertion). Also, there were no avulsion failures in any of the ligaments, which are sometimes seen by other researchers. This suggests that the failure mechanism is not sensitive to loading rate, and that the testing orientation (distraction with 0° of flexion) permitted repeatable failures.

The ATOS^{TM} system has been widely used for digitization of non-biological objects for use in CAD and rapid prototyping (Capture 3d, 2002) as well as for digitization of ligament surfaces (Bose *et al*. 2002). The results of the surface digitizations in this study show high variation in ligament cross-sectional area. This is an obvious indicator of the potential for interspecimen variability. Since stress is calculated as force per unit area, and we assume that the resultant force lies along the line that connects the geometric centers of the insertions; the contours selected for stress calculation were those perpendicular to this line (Figure 5). This assumption has been widely used by other researchers (Trent *et al.* 1976, Kennedy *et al.* 1976, Noyes & Grood 1976, Marinozzi *et al*. 1983, Butler *et al.* 1986, Woo *et al.* 1991), but its validity is still unknown to us.

The accuracy of the LSAD relationships for the specimens tested at the high rate is debatable since there were no data points to help define the curve at strains higher than 10% (normal linear strain). The original intention was to use the high speed video images to augment the LSAD relationship; however, the images lacked sufficient resolution to calculate strains with acceptable accuracy. An assumption made when calculating strains in the manner described above is that the strain on the

surface of the ligament is the same as the strains within the ligament that govern failure. The validity of this assumption is higher for LCL specimens than for MCL specimens since the shortest fibers of the MCL are on the lateral side of the ligament, whereas the photographs were taken from the medial side because the lateral view of the ligament during testing was too small to accurately track speckle pattern changes.

The data in Table 3 show that most of the properties vary widely within each group. This variation can be somewhat attributed to the varying ages of the specimens (40-66 years). Data published by Woo *et al.* (1991) suggest that the ultimate load of an ACL from a 40 year old PMHS could be as much as 200% greater than that of an ACL from a 60 year old PMHS, whereas the linearized ACL stiffness (load per unit displacement) was only up to 20% higher in a 40 year-old than in a 60 year-old PMHS. However, although our data are not averaged for age group, it appears that our results do not depict such a large difference in variations of stiffness (and modulus) values as compared to variations in ultimate load (or stress) values.

The most important conclusion to draw from the data presented in this study is the difference in stress-strain relationship between each ligament tested at the low rate as compared to the same type of ligament tested at the high rate (Figures 6 and 7). The regression analysis confirms that both the MCL and LCL have a rate sensitive constitutive relationship over the range of strain-rates examined in this study (1%/s-2400%/s).

The most interesting feature of the data presented in this study is that both the elastic modulus and the stress at maximum force are, on average, higher in the LCL than in the MCL. We feel that this is because each LCL was entirely loaded (all of its fibers were bearing load) whereas each MCL was not (only some of its fibers were bearing the load). The small size and relatively simple orientation of the fibers of the LCL allowed for the entire ligament to bear the load in the distraction orientation. However, the MCL structure is much more complex; the tibial insertion of the MCL in some cases was as long as 10 cm, and the ligament itself consists of multiple layers or bands of fibers that weave together. The complex structure of the MCL prohibited loading of all of the fibers of the MCL in distraction at 0° flexion. This partial-loading results in the surface digitizer over estimating the loaded area of the ligament, and thus underestimating the ultimate stress and elastic modulus. Partial-loading of the MCL also explains why while LCLs have greater linearized elastic moduli, yet they have lower linearized distraction stiffnesses than MCLs.

Another interesting feature of the data is that the Lagrangian strain at maximum force is, on average, lower in the LCLs than in the MCLs for both high and low rate tests. The Lagrangian strain-rates applied to the ligaments tested at the high rate are less, yet they were still of the same order of magnitude as the goal (3000-5000 %/s) strain-rates (those predicted to be applied to the collateral ligaments of pedestrians during a lateral impact PAC).

CONCLUSIONS

- The strain-rates achieved experimentally in this study are of the same order of magnitude as those expected to occur in pedestrian collateral ligaments in a lateral aspect PAC at 40 km/h.
- The data show that in both the LCL and the MCL, the stress at a particular strain in an average high rate test is significantly greater than the stress at the same strain in an average low rate test ($p<0.001$) implying ligaments have rate-dependent properties.
- The average LCL ultimate stress and elastic modulus (39.3 MPa and 477.9 MPa, respectively) are more than double the ultimate stress and elastic modulus of the MCL (15.98 and 138.3, respectively).
- The Lagrangian strain at maximum force is, on average, lower in the LCLs than in the MCLs tested at both a high rate (10.5% and 11.47%, respectively) and a low rate (7.14% and 20.32%).
- The average maximum force and distraction stiffness are greater for the MCL than for the LCL.

REFRENCES

Allard, P., Thirty, P.S., Bourgault, A., and Drouin, G. "Pressure Dependence of the Area Micrometer Method in Evaluation of Cruciate Ligament Cross Section". *Journal of Orthopaedic Research*, Vol 1, pp. 265-267, 1979.

Beillas, P., Begeman, P.C., Yang, K.H., King, A.I., Arnoux, P-J., Kang, H-S., Kayvantash, K., Brunte, C., Cavallero, C., and Prasad, P. "Lower Limb: Advanced FE Model and New Experimental Data". *Stapp Car Crash Journal*, pp. 469-494, 2001.

Bermond, F., Ramet, M., Bouquet, R., and Cesari, D. "A Finite Element Model of the Pedestrian Knee-Joint in Lateral Impact". *International Conference on the Biomechanics of Impacts (IRCOBI)*, 1993.

Bermond, F., Ramet, M., Bouquet, R., and Cesari, D. "A Finite Element Model of the Pedestrian Leg in Lateral Impact". *14th International Conference on the Enhanced Safety of Vehicles (ESV)*. 1994.

Bhalla, K., Bose, K., Madeley, N.J., Kerrigan, J., Crandall, J., Longhitano, D., and Takahashi, Y. "Evaluation of the Response of Mechanical Pedestrian Knee Joint Impactors in Bending and Shear Loading". *18th ESV*, 2003.

Bose, D., Sanghavi, P., Kerrigan, J.R., Madeley, N.J., Bhalla, K.S., and Crandall, J.R. "Material Characterization of Ligaments Using Non-Contact Strain Measurement and Digitization". *Injury Biomechanics Research, Proceedings of the Thirtieth International Workshop.* 2002.

Bunketorp, O., Aldman, B., Thorngen, L., and Romanus B. "Clinical and Experimental Studies on Leg Injuries in Car-Pedestrian Accidents". *Biomechanics of impact injury and injury tolerance of the extremities, Society of Automotive Engineer.* Warrendale, Pennsylvania, USA, S.H Backaitis (Editor), *PT-56*, pp. 699-710, 1996.

Butler, D.L., Kay, M.D., Stouffer, D.C. "Comparison of Material Properties in Fascicle-Bone Units from Human Patellar Tendon and Knee Ligaments. *Journal of Biomechanics*, 19(6), pp. 425-432, 1986.

Butler, D.L., Grood, E.S., Noyes, F.R., Zernickes, R.F., and Brackett, K. "Effects of the Structure and Strain Measurement Technique on the Material Properties of Young Human Tendons and Fascia". *J. Biomechanics,* 17, pp. 579-596, 1984.

CAPTURE 3D at the website http://www.capture3d.com/quality-en.pdf.

Commision of the European Communities, "Proposal for a Directive of the European Parliament and of the Council Relating to the Protection of Pedestrians and Other Vulnerable Road Users in the Event of a Collision with a Motor Vehicle and Amending Directive 70/156/EEC". Downloaded: http://europa.eu.int/comm/enterprise/automotive/pagesbackground/pedestrianprotection/index.htm, on February 9, 2003.

Funk, J.R., Hall, G.W., Crandall, J.R., and Pilkey, W.D. "Linear and Quasi-linear Viscoelastic Characterization of Ankle Ligaments". *Journal of Biomechanical Engineering*, Vol 122, pp. 15-22, 2000.

Haut, R.C., and Little, R.W. "Rheological Properties of Canine Anterior Cruciate Ligaments". *J. Biomechanics*, Vol 2, pp. 289-298, 1969.

Hollis, J.M., Lyon, R.M., Marcin, S., Horibe, E.B., Lee, Woo, S.L.Y. "Effect of Age and Loading Axis on the Failure Properties of the Human ACL". *Transactions of the Orthopaedic Research Society*, 13, pp. 81, 1988.

Iconis, F., Steindler, R., and Marinozzi, G. "Measurement of Cross Sectional Area of Collagen Structures (Knee Ligaments) by Means of an Optical Method". *J. Biomechanics*, 20(10), pp. 1003-10, 1987.

Jones, R.S., Nawana, N.S., Pearcy, M.J., Learmonth, D.J.A., Bickerstaff, D.R., Costi, J.J., Paterson, R.S. "Mechanical Properties of the Human Anterior Cruciate Ligament". *Clinical Biomechanics*, 10(7), pp. 339-344, 1995.

Kajzer, J., Cavallero, S., Ghanouchi, S., Bonnoit, J., Aghorbel. "Response of the Knee Joint in Lateral Impact: Effect of Shearing Loads, *IRCOBI*, pp. 293-304, 1990.

Kajzer, J., Cavallero, S., Bonnoit, J., Morjane, A., Ghanouchi, S. "Response of the Knee Joint in Lateral Impact: Effect of Bending Moment". *IRCOBI*, 1993.

Kajzer, J., Schroeder, G., Ishikawa, H., Matsui, Y., Bosch, U., "Shearing and Bending Effects at the Knee Joint at High Speed Lateral Loading," *Society of Automotive Engineers,* SAE Paper 973326, 1997.

Kajzer, J., Ishikawa, H., Matsui, Y., Schroeder, G., Bosch, U., "Shearing and Bending Effects at the Knee Joint at Low Speed Lateral Loading," *Society of Automotive Engineers,* SAE Paper 1999-01-0712, 1999.

Kennedy, J.C., Hawkins, R.J., Willis, R.B., Danylchuck, K.D. "Tension Studies of Human Knee Ligaments. Yield Point, Ultimate Failure, and Disruption of the Cruciate and Tibial Collateral Ligaments". *Journal of Bone and Joint Surgery,* American Volume 58(3), pp. 350-355, 1976.

Kerrigan, J.R., Bhalla, K.S., Madeley, N.J., Funk, J.R., Bose, D., Crandall, J.R. "Experiments for Establishing Pedestrian-Impact Lower Limb Injury Criteria". *Society of Automotive Engineers*, SAE Paper 2003-01-0895, 2003.

Lee, T.Q., and Woo, S.L.Y. "A New Method for Determining Cross Sectional Shape and Area of Soft Tissues. *J. Biomechanical Eng.*, 110, pp. 110-114, 1988.

Maeno, T., and Hasegawa, J. "Development of a Finite Element Model of the Total Human Model for Safety (THUMS) and Application to Car-Pedestrian Impacts". *17th ESV*, 2001.

Marinozzi, G., Pappalardo, S., Steindler, R. "Human Knee Ligaments: Mechanical Tests and Ultrastructural Observations". *Italian Journal of Orthopaedics and Traumatology*, 9(2), pp. 231-240, 1983.

National Highway Traffic Safety Administration, "Traffic Safety Facts 2001-Pedestrians", *DOT HS 809 478*, 2001.

Noyes, F.R., Grood, E.S. "The strength of the anterior cruciate ligament in humans and Rhesus monkeys". *Journal of Bone Joint Surgery*, American Volume 58(8), pp. 1074-1082, 1976.

Piziali, R.L., Rastegar, J., Nagel, D.A., Schurman, D.J. "The Contribution of the Cruciate Ligaments to the Load-Displacement Characteristics of the Human Knee Joint". *Journal of Biomechanical Engineering*, 102(4), pp. 277-283, 1980.

Rauch, G., Allzeit, B., Gotzen, L. "Biomecahnische Untersuchungen zur Zugfestigkeit des vorderen Kreuzbandes unter besonderer Berücksichtigung der Altersabhängigkeit". *Unfallchirurg* 91(10), pp. 437-443, 1988.

Rowden, N.J., Sher, D., Rogers, G.J., Schindhelm, K. "Anterior Cruciate Ligament Graft Fixation. Initial Comparison of Patellar Tendon and Semitendinosus Autografts in Young Fresh Cadavers". *American Journal of Sports Medicine*, 25(4), pp. 472-478, 1997.

Schuster, P.J., Chou, C.C., Prasad, P., Jayaraman, G. "Development and Validation of a Pedestrian Lower Limb Non Linear 3D Finite Element Model". *Stapp Car Crash Journal*, 44, 2000.

Takahashi, Y., Kikuchi, Y., Konosu, A., Ishikawa, H. "Development and Validation of the Finite Element Model for the Human Lower Limb of Pedestrians, *Stapp Car Crash Journal*, 44, 2000.

Takahashi Y., Kikuchi Y. Personal Communication, 2002.

Takahashi Y., Kikuchi, Y., Mori, F., and Konosu, A., "Advanced FE Lower Limb Model for Pedestrians". *18th ESV*, 2003.

Teresinski, G., and Madro, R. "Knee Joint Injuries as a Reconstructive Factor in Car-to-Pedestrian Accidents". *Forensic Science International,* 124, pp. 74-82, 2001.

Tremblay, G.R., Laurin, C.A., Drovin, G. "The Challenge of Prosthetic Cruciate Ligament Replacement." *Clinical Orthopaedics and Related Research*, **(**147), pp. 88-92, 1980.

Trent, P.S., Walker, P.S., Wolf, B. "Ligament Length Patterns, Strength, and Rotational Axes of the Knee Joint". *Clinical Orthopaedics and Related Research* (117), pp. 263-270, 1976.

Woo, S.L.Y., Hollis, J.M., Adams, D.J., Lyon, R.M., Takai, S. "Tensile Properties of the Human Femur-Anterior Cruciate Ligament-Tibia Complex. The Effects of Specimen Age and Orientation." *American Journal of Sports Medicine*, 19(3), pp. 217-225, 1991.

Woo, S.L.Y., Danto, M.I., Ohland, K.J., L., T.Q., and Newton, P.O. "The Use of a Laser Micrometer System to Determine the Cross-Sectional Shape and Area of Ligaments: A Comparative Study with Two Existing Methods". *J. Biomechanical Eng.,* 112, pp. 426-431, 1990.

Yang, J.K., Wittek, A., Kajzer, J. "Finite Element Model of the Human Lower Extremity Skeleton System in Lateral Impact". *IRCOBI*, 1996.